ROCKY MOUNTAIN
JOURNAL OF MATHEMATICS
Volume 30, Number 3, Fall 2000

# ENFORCED DRAINAGE TERRAIN MODELS USING MINIMUM NORM NETWORKS AND SMOOTHING SPLINES

LEONOR MALVA AND KĘSTUTIS ŠALKAUSKAS

ABSTRACT. Some techniques to overcome the problem of enforced drainage in mathematical terrain modeling are presented. Data available about the terrain consist of a set of scattered benchmarks and an idealized, piecewise linear hydrographic net. First, a cubic spline minimum norm network, MNN, on a triangulation of the benchmark data is created, in order to create a first impression of the terrain. The cubics from the MNN supply temporary profiles along the edges of the triangulation; these are modified on those edges which intersect the hydrographic net in order to simulate erosion of the terrain. This is done by weighted smoothing spline techniques. A network of monotonic cubic arcs is created on the edges of the hydrographic net. To arrive at the final surface model, a blending method is applied that requires the specification of elevations and gradient vectors along all edges. Although the elevations along the edges that lie in the hydrographic net are monotonic by construction, the gradient there should also be parallel to the direction of the hydrographic net. This is achieved approximately in an $L^2$-sense. The result is a differentiable surface which interpolates the stream channels as well as the modified spline MNN.

**1. Introduction.** An important problem in mathematical terrain modeling is that of enforced drainage. Terrain models based on topographic benchmark data often suffer from undulations and this results in "dams" and associated pools forming in what should be stream channels. In part, this is the result of not constraining the terrain model to honor the hydrographic net. We will develop some techniques that help to overcome this problem. Our approach was motivated by aerial observation of some prairie terrain in western Canada. It was strikingly evident that an underlying, slowly undulating surface was eroded by systems of streams, and that a terrain model based solely on point data

Received by the editors on May 25, 1998, and in revised form on July 30,1999.
The research of the first author was supported in part by the Calouste Gulbenkian Foundation and by a NATO Fellowship Portugal, ref. 3/A/96/PO.
The work of the second author was supported in part by NSERC Canada grant OGP0008521.

such as elevations or even gradients at benchmarks would most likely be unsatisfactory. We therefore include a simplified hydrographic net as data. Any method that honors the hydrographic net must do so to the extent of interpolating some of its elevations and the preservation of monotonicity. It is possible to achieve this simply by triangulating all data locations in such a way that the (simplified) hydrographic net lies along edges. Linear interpolation on the triangles yields a surface that interpolates all Lagrangian point data and preserves the monotonicity of the net. It does so at the cost of smoothness. Nevertheless, this method has been employed by geographers [**10**].

The method developed here yields a $C^1$ surface whose shape can be influenced to some extent by the user making adjustments to some parameters locally. As well, we insist on preserving not just point properties of the hydrographic net but its monotonicity as well. It does not appear possible to satisfy such requirements by using methods based solely on minimization of functionals such as thin-plate splines or smoothing splines on $\mathbf{R}^2$. Figure 6 is a contour map of a thin-plate spline surface that interpolates benchmark elevations as well as elevations of the hydrographic net at selected confluences and should be compared with a result of applying our method shown in Figures 7–9. We have used only 9 benchmark points and 11 points on the hydrographic net taken from Figure 10. The thin-plate spline is very smooth but does not capture the main features of the hydrographic net or the original contour map. This is especially evident in the eastern part of the map. Our approach leads to noisier surfaces which, however, conform better to the original, especially in view of the sparse data.

In Section 2 we describe our assumptions about the data set to which our method can be applied. In Section 3 we begin the method with a short review of a minimum norm network, MNN, of cubic arcs [**8**], [**5**] defined on a triangulation of benchmarks and interpolating the benchmark elevations. A smooth, uneroded surface could be realized by applying a blending method such as the side vertex method [**7**] or the finite element method discussed in [**1**]. The hydrographic net is modeled by a set of vertices and edges that form a tree, in the graph-theoretic sense, in the coordinate plane, together with monotonic cubic elevations constructed in Section 4 on the edges of the net by the techniques in [**4**]. The MNN is then merged with the hydrographic net by simulating some erosion of the MNN on those edges of the

triangulation that intersect the edges of the net. For this we use a family of weighted smoothing splines constructed in Section 5 and an erosion model presented in Section 6. This modifies the cubic profile coming from the MNN to correspond with the hydrographic net. By constructing a family of weighted smoothing splines on each such edge, we are able to avoid undershoot in the modified profile, and some user interaction is allowed. The hydrographic net then contributes additional edges to the original triangulation, and cubic arcs are defined on all edges. Finally, in our illustration of the method, the entire curve network is blended by the side vertex method. For this it is necessary to define a gradient on every edge. This is discussed in Section 7, where we interpolate gradients known at the vertices and take some care that the interpolated gradient is close in direction to the hydrographic net in an $L^2$ sense on the appropriate edges.

**2. Preliminaries.** We assume that the data available about the terrain consist of two sets. One is a set $\mathcal{B} := \{x_i, y_i, z_i\}_1^N$ of scattered benchmarks consisting of the set of "vertices," $\mathcal{V} := \{V_i = (x_i, y_i)\}_1^N$ together with the corresponding elevations $z_i$. A triangulation of these vertices will have a set of edges, say $\mathcal{E}$. Let $\Omega$ denote the convex hull of $\mathcal{V}$. A system of streams (including their elevations) located in $\Omega$ will be called a 3D-hydrographic net. Its projection on the coordinate plane will be simply called a hydrographic net. Our second data is an idealized 3D-hydrograhpic net whose (idealized) hydrographic net $\mathcal{H}$ is assumed to have the appearance of a tree, in the graph-theoretic sense, with elevations defined at its vertices. $\mathcal{H}$ is to be a reasonable approximation to the physical net, and we assume that we have some freedom in how to choose it. In particular, we assume that the physical hydrographic net cuts any edge of a triangulation at at most one point interior to the edge, and that the idealized net $\mathcal{H}$ has its vertices only on the edges at precisely these crossing points. We seek a $C^1$ surface $S : \Omega \to \mathbf{R}$ such that $S(x_i, y_i) = z_i$, $i = 1, \ldots, N$, and whose restriction to the net $\mathcal{H}$ is monotonic and interpolates its elevation.

Figures 1(a), (b) and (c) illustrate a typical triangulation of $\mathcal{V}$, an approximate hydrographic net $\mathcal{H}$ and their superposition.

**3. The spline minimum norm network.** Spline minimum norm networks are discussed in some generality in [**8**], [**5**] and [**9**]. For our

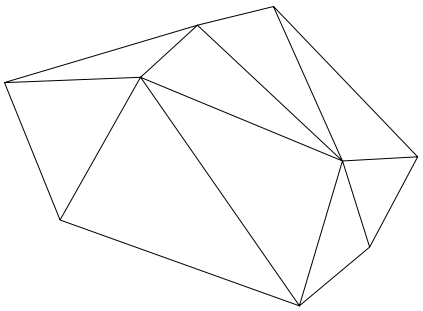

(a) The triangulation $\mathcal{E}$.

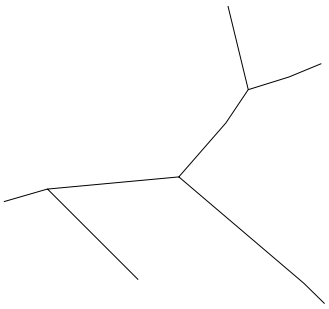

(b) The hydrographic net $\mathcal{H}$.

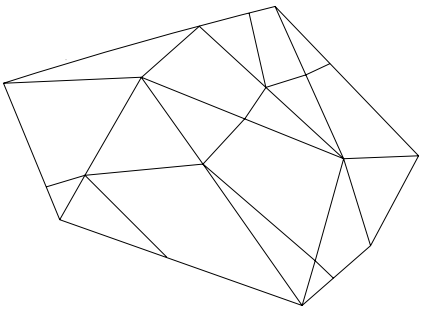

(c) $\mathcal{E} \cup \mathcal{H}$.

FIGURE 1.

purposes it will be sufficient to describe such a network as follows. The points of $\mathcal{V}$ are used as vertices of a triangulation of the domain $\Omega$. Let $\mathcal{E}$ be the set of edges of the triangulation. The minimum norm network is a set of cubic arcs, each defined on an edge, that interpolate the given elevations at the vertices of the triangulation. The arcs meeting at a vertex are tangent to one and the same plane, and the gradients of all such planes are determined by minimizing an energy semi-norm. Specifically, in the simplest notation, if $e$ is an edge in $\mathcal{E}$, $f$ is a cubic arc on $e$ and $t$ is the arc length along $e$, the gradients are chosen to minimize

$$\sum_{e\in\mathcal{E}} \int_e [f''(t)]^2\, dt.$$

Holland [**5**] provides for a weighted semi-norm for additional control of the shape of the MNN.

We focus on a typical triangle with vertices $V_i, V_j, V_k$. Let $l_{ij}$ be the length of the edge connecting $V_i$ to $V_j$. If the minimum norm network is regarded as the restriction to $\mathcal{E}$ of a certain $C^1$ function $S : \Omega \to \mathbf{R}$, the required gradients at the vertices are $\nabla S_i = (S_x(V_i), S_y(V_i))$, $1 \le i \le N$. Let $N_i$ denote the set of index pairs $i, j$ for edges emanating from $V_i$. In [**8**] these are shown to satisfy

$$\sum_{ij\in N_i} \frac{(x_j - x_i)}{l_{ij}^3} \Bigg[ (x_j - x_i) S_x(V_i) + (y_j - y_i) S_y(V_i) + \frac{(x_j - x_i)}{2} S_x(V_j) + \frac{(y_j - y_i)}{2} S_y(V_j) + \frac{3(z_i - z_j)}{2} \Bigg] = 0,$$

$$\sum_{ij\in N_i} \frac{(y_j - y_i)}{l_{ij}^3} \Bigg[ (x_j - x_i) S_x(V_i) + (y_j - y_i) S_y(V_i) + \frac{(x_j - x_i)}{2} S_x(V_j) + \frac{(y_j - y_i)}{2} S_y(V_j) + \frac{3(z_i - z_j)}{2} \Bigg] = 0.$$

See [**5**] for generalizations of this to weighted semi-norms and other bases. Figure 2 illustrates an unweighted MNN for data defined at the benchmarks used for Figure 1(a).

**4. An elevation system for the hydrographic net.** We now propose a method for generating an elevation system for the

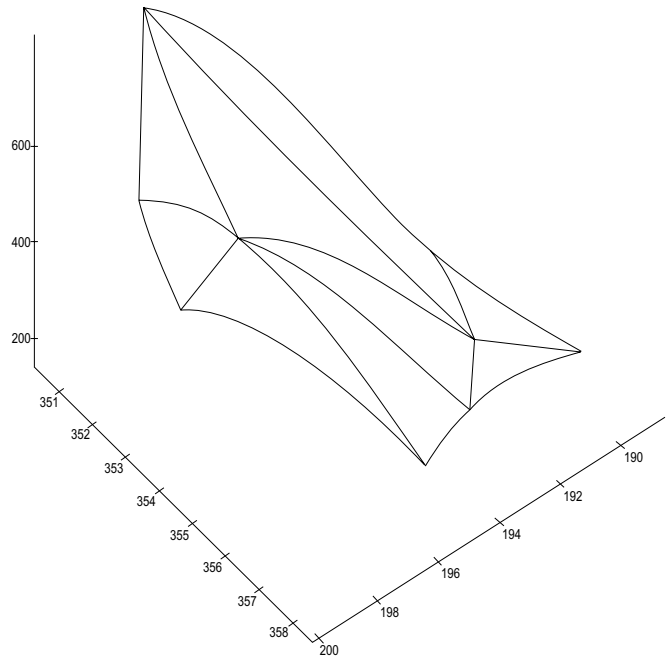


FIGURE 2. A minimum norm network.

hydrographic net with the property that, on any connected subgraph of $\mathcal{H}$ not containing a confluence in its interior, the elevation is a $C^1$ piecewise cubic (in arc length) which interpolates the given elevations at the vertices and is monotonically increasing in the upstream direction. Confluences can be regarded as initial points of such connected graphs. Thus, an elevation system can be generated for the entire net $\mathcal{H}$ and, with $\mathcal{H}$, constitutes the idealized 3D-hydrographic net. We will make use of the results of Fritch and Carlson [**4**].

Recall our assumption that the hydrographic net has its vertices only on the interiors of the edges of the triangulation. At each vertex one has to ensure consistency in the sense that the various curves of a 3D-net meeting there correspond to a unique tangent plane. In addition, the gradient of the tangent plane should be approximately parallel to the hydrograhic net at the vertex. We say "approximately" because the edges entering the vertex need not be collinear. This places a restriction

on the gradients of the underlying surface at the vertices of the net, and we pursue this next.

Consider a connected subgraph of $\mathcal{H}$ with $n$ vertices and no interior confluences. Denote the vertices consecutively $P_i$, $1 \le i \le n$, in the (positive) upstream direction. (It will be convenient to regard the $\mathbf{P}_i$ as position vectors.) Let $\tilde{S}$ be an elevation function, i.e., the restriction of $S$ to the subgraph, on this portion of the stream, and let $t$ be the arclength parameter along edges of $\mathcal{H}$.

**Proposition 4.1.** *There are constants $A_i > 0$ such that*

$$\frac{\partial}{\partial t}\tilde{S}(\mathbf{P}_i^+) = A_i \frac{\partial}{\partial t}\tilde{S}(\mathbf{P}_i^-), \quad 2 \le i \le n-1,$$

*and the valley profile and stream are tangent to one and the same surface at the vertex $\mathbf{P}_i$.*

*Proof.* Let $\mathbf{a} = (a_1, a_2) = (\mathbf{P}_i - \mathbf{P}_{i-1})/\|\mathbf{P}_i - \mathbf{P}_{i-1}\|$ and $\mathbf{b} = (b_1, b_2) = (\mathbf{P}_{i+1} - \mathbf{P}_i)/\|\mathbf{P}_{i+1} - \mathbf{P}_i\|$ be unit tangent vectors along the edges of $\mathcal{H}$ at $\mathbf{P}_i$ in the positive (upstream) direction and $\mathbf{c} = (c_1, c_2)$ a unit vector approximately perpendicular to net. Denote by $\nabla S_i$ the gradient of the underlying surface $S$ at $\mathbf{P}_i$.

The directional derivatives of $S$ at the intersection point are

$$\begin{aligned} D_{\mathbf{a}}S(\mathbf{P}_i) &= \frac{\partial}{\partial t}\tilde{S}(\mathbf{P}_i^-) = \nabla S_i \cdot \mathbf{a}, \\ D_{\mathbf{b}}S(\mathbf{P}_i) &= \frac{\partial}{\partial t}\tilde{S}(\mathbf{P}_i^+) = \nabla S_i \cdot \mathbf{b}, \\ D_{\mathbf{c}}S(\mathbf{P}_i) &= \nabla S_i \cdot \mathbf{c} = 0. \end{aligned} \tag{4.1}$$

Solving the first and last of these for the components of $\nabla S_i$, we find

$$\frac{\partial S(\mathbf{P}_i)}{\partial x} = \frac{c_2(\partial/\partial t)\tilde{S}(\mathbf{P}_i^-)}{\begin{vmatrix} a_1 & a_2 \\ c_1 & c_2 \end{vmatrix}}, \qquad \frac{\partial S(\mathbf{P}_i)}{\partial y} = -\frac{c_1(\partial/\partial t)\tilde{S}(\mathbf{P}_i^-)}{\begin{vmatrix} a_1 & a_2 \\ c_1 & c_2 \end{vmatrix}}.$$

Now

$$D_{\mathbf{b}}S(\mathbf{P}_i) = \nabla S_i \cdot \mathbf{b} = \frac{\begin{vmatrix} b_1 & b_2 \\ c_1 & c_2 \end{vmatrix}}{\begin{vmatrix} a_1 & a_2 \\ c_1 & c_2 \end{vmatrix}} \frac{\partial}{\partial t}\tilde{S}(\mathbf{P}_i^-),$$

and

$$A_i = \frac{\begin{vmatrix} b_1 & b_2 \\ c_1 & c_2 \end{vmatrix}}{\begin{vmatrix} a_1 & a_2 \\ c_1 & c_2 \end{vmatrix}}. \tag{4.2}$$

Extending $\mathbf{a}, \mathbf{b}, \mathbf{c}$ to $\mathbf{R}^3$,

$$\mathbf{a} \times \mathbf{c} = \left(0, 0, \begin{vmatrix} a_1 & a_2 \\ c_1 & c_2 \end{vmatrix}\right),$$
$$\mathbf{b} \times \mathbf{c} = \left(0, 0, \begin{vmatrix} b_1 & b_2 \\ c_1 & c_2 \end{vmatrix}\right).$$

But $\mathbf{a} \times \mathbf{c}$ and $\mathbf{b} \times \mathbf{c}$ have the same direction, consequently, $A_i > 0$. □

It follows that, given a stream gradient at the upstream end of a segment of $\mathcal{H}$, we have a unique gradient at the downstream end of the next *upstream* segment. It is only necessary to make a choice for $\mathbf{c}$. In our examples we choose $\mathbf{c}$ as follows. Because the edges entering the vertex need not be collinear, we take $\mathbf{c}$ orthogonal to $(\mathbf{a}+\mathbf{b})/2$. In the next result we will show that the slopes at the upstream ends of the segments can be determined so that $\tilde{S}$ is not only $C^1$ but monotonically increasing as well.

Following [**4**], let

$$\Delta_i = \frac{\tilde{S}(\mathbf{P}_{i+1}) - \tilde{S}(\mathbf{P}_i)}{\|\mathbf{P}_i - \mathbf{P}_{i+1}\|},$$
$$\alpha_i = \frac{1}{\Delta_i}\frac{\partial}{\partial t}\tilde{S}(\mathbf{P}_i^+), \qquad \beta_i = \frac{1}{\Delta_i}\frac{\partial}{\partial t}\tilde{S}(\mathbf{P}_{i+1}^-), \tag{4.3}$$

be the normalized slopes at the ends of the segment $\mathbf{P}_i\mathbf{P}_{i+1}$, $1 \le i \le n-1$. According to [**4**], a cubic segment of $\tilde{S}$ on $\mathbf{P}_i\mathbf{P}_{i+1}$ is monotonically increasing if the point $(\alpha_i, \beta_i) \in \mathcal{M}$ where $\mathcal{M}$ is a certain set in $\mathbf{R}^2$, see Figure 3. From Proposition 4.1, the differentiability constraints have the form

$$\frac{\partial}{\partial t}\tilde{S}(\mathbf{P}_i^+) = A_i \frac{\partial}{\partial t}\tilde{S}(\mathbf{P}_i^-),$$

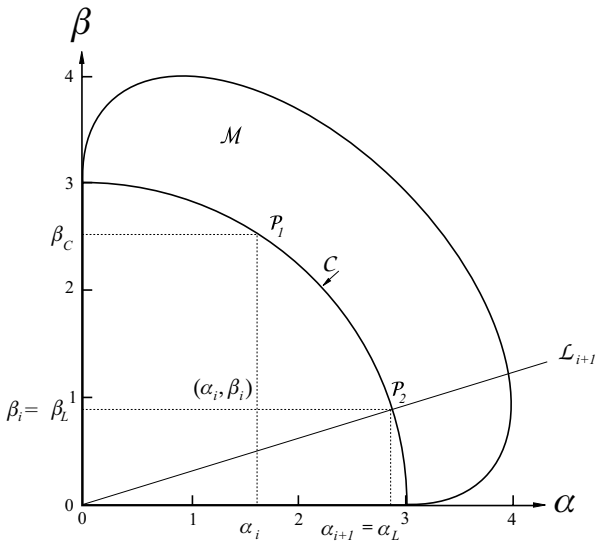


FIGURE 3. Determining slopes for monotonicity.

or equivalently,

$$\alpha_i = \mu_i \beta_{i-1} > 0, \quad 2 \le i \le n-1,$$

where

$$\mu_i = \frac{\Delta_{i-1}}{\Delta_i} A_i. \tag{4.4}$$

We will show that, given an admissible $\alpha_1, \beta_1$ and the entire set $(\alpha_i, \beta_i)$, $2 \le i \le n-1$ can be chosen to satisfy both the monotonicity and differentiability constraints for the entire subgraph. The essentials of the approach can be found in [**4**].

**Proposition 4.2.** *On any subgraph of $\mathcal{H}$ with $n$ vertices, a river elevation function $\tilde{S}$ exists which is monotonically increasing and satisfies the constraints at the vertices.*

*Proof.* We proceed by constructing an algorithm. As in [**4**], let $\mathcal{S}$ be a subset of $\mathcal{M}$ that satisfies

$$(\alpha, \beta) \in \mathcal{S} \quad \text{and} \quad 0 \le \alpha^* \le \alpha, 0 \le \beta^* \le \beta \Longrightarrow (\alpha^*, \beta^*) \in \mathcal{S}$$

and has positive area.

It is easily seen by examining the region $\mathcal{M}$ (see Figure 3) [**4**] that $\mathcal{S}$ is bounded by the line segments $\alpha = 0$, $0 \le \beta \le 3$, $\beta = 0$, $0 \le \alpha \le 3$ and some suitable continuous curve $\mathcal{C}$ connecting the points (0,3) and (3,0) on the boundary of $\mathcal{M}$. Note that the lines $\mathcal{L}_i : \alpha = \mu_i \beta$, $1 \le i \le n-1$ (4.4) pass through the origin, have positive slope since (4.2) $A_i > 0$ and have a segment of positive length in $\mathcal{S}$.

For the following argument it may be helpful to refer to Figure 3. Suppose $\alpha_i \in (0,3)$ for some $i$ satisfying $1 \le i \le n-1$. Let $\mathcal{P}_1 = (\alpha_i, \beta_C)$ be the point on $\mathcal{C}$, and let $\mathbf{P}_2 = (\alpha_L, \beta_L)$ be the point of intersection of $\mathcal{L}_{i+1}$ and $\mathcal{C}$. Observe that $\alpha_L \in (0,3)$. Let $\beta_i = \min\{\beta_C, \beta_L\}$. Since $(\alpha_i, \beta_i) \in \mathcal{S}$, the corresponding segment of $S$ is monotonic. Now put $\alpha_{i+1} = \mu_{i+1}\beta_i$. If $\beta_i = \beta_L$, then $\alpha_{i+1} = \alpha_L \in (0,3)$. On the other hand, if $\beta_i = \beta_C \le \beta_L$, then by the monotonicity of $\mathcal{L}_{i+1}$ we have $\alpha_{i+1} \le \alpha_L \in (0,3)$. We conclude that $\alpha_i \in (0,3)$ implies $\alpha_{i+1} \in (0,3)$.

It follows that, for an initial choice $\alpha_1 \in (0,3)$ and $\mathcal{C}$, there are determined $\beta_1$ and a set of pairs $(\alpha_i, \beta_i)$, $2 \le i \le n-1$, such that the stream elevation function $\tilde{S}$ is monotonically increasing and satisfies the smoothness constraints at the vertices. □

We may make use of this proposition to generate a set of cubic arcs on all edges of $\mathcal{H}$. At the lowest point of $\mathcal{H}$ choose $\alpha_1 \in (0,3)$. The algorithm of Proposition 4.2 determines the slopes of the elevation function by (4.3) as far as the first confluence point, say $\mathbf{P}_n$. There, $\beta_{n-1} = (\partial/\partial t)\tilde{S}(\mathbf{P}_n^-)/\Delta_{n-1}$. Now there will be a set of different lines of the form $\mathcal{L}_n : \alpha = \mu_n \beta$, one for each new subgraph of $\mathcal{H}$ originating there, one direction vector $\mathbf{a}$, several associated direction vectors $\mathbf{b}$ and corresponding vectors $\mathbf{c}$. If equations in (4.1) are used with different $\mathbf{b}$'s and $\mathbf{c}$'s, a unique gradient will not result. We therefore take for $\mathbf{b}$ the average of the upstream direction vectors of the tributaries and then take $\mathbf{c}$ orthogonal to $(\mathbf{a} + \mathbf{b})/2$. Next we use Proposition 4.1 to determine directional derivatives on all streams joining there; each is an $\alpha_1$ for the subgraph in question. In this way we determine a cubic arc network on $\mathcal{H}$. The very first value $\alpha_1$ remains a parameter and the curve $\mathcal{C}$ is at the disposal of the user. We can also determine gradients of an underlying surface at the vertices of $\mathcal{H}$. These will be needed

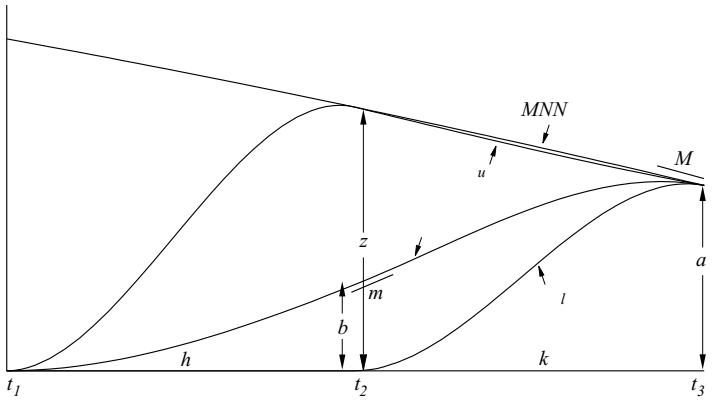


FIGURE 4. Smoothing splines.

for the blending of the entire curve network on $\mathcal{E}$ and on the edges in $\mathcal{H}$ and can be obtained by solving the second pair of the equations in (4.1). By this choice, the special situation at an initial point of $\mathcal{H}$ is accommodated.

**5. Smoothing splines.** We will use simple smoothing splines in an erosion model in order to merge the curve network of the MNN with the curve network on $\mathcal{H}$ constructed in the previous section. The idea is to modify a temporary terrain profile obtained from the MNN in a way that stimulates the erosion of the terrain to the elevation and slope of the stream. This yields a profile for the valley containing the stream. A family of weighted smoothing splines is constructed that avoids undershoot in the modified profile and allows some user interaction in controlling the nature of the erosion.

Smoothing splines are well known, but we will use weighted smoothing splines, and we develop some of their properties in this section.

We approach the weighted smoothing spline by recalling the simplest weighted splines introduced for one variable functions by Šalkauskas [**11**] and Cinquin [**3**] as solutions to the problem of finding

$$f \in H[a,b] := \{f \mid f' \text{ is absolutely continuous in } [a,b] \text{ and } f'' \in L^2[a,b]\}$$

which interpolates given values $f_i$ at a set of knots $a = t_1 < \cdots < t_n = b$

and minimizes the weighted "energy" functional

$$J(f) = \int_a^b w(t)[f''(t)]^2\,dt.$$

Here $w > 0$ is a step function which may depend on the data with possible discontinuities only at the knots. A classical smoothing spline [**12**], [**6**] does not have to interpolate and minimizes

$$Q(f) = \int_a^b [f''(t)]^2\,dt + \alpha \sum_{i=1}^{n} (f_i - f(t_i))^2$$

over $f \in H[a,b]$ for a fixed $\alpha \in [0,\infty)$. The unique optimum is a certain cubic spline. As in $J$, a weight function can be included for additional shape control. Here we will only need the simplest setting for these splines, and we will derive some special properties needed for our application. We restrict $f$ to a small space of functions and work with few knots and special boundary conditions.

Let $\{\phi_i, \psi_i\}$, $i = 1, 2, 3$, be the Hermite cardinal functions for ordinate and derivative interpolation at knots $t_1 < t_2 < t_3$. Then a piecewise cubic function $s$ interpolating zero data at $t_1$, whose value at $t_2$ is $b$ and derivative there is $m$, and which interpolates ordinate and slope $a$ and $M$ respectively at $t_3$, can be written as

$$s = b\phi_2 + m\psi_2 + a\phi_3 + M\psi_3 \tag{5.1}$$

on $[t_1, t_3]$. See Figure 4.

**Proposition 5.1.** *For any nonnegative weight function $w$ which is not identically zero, is constant on the intervals $[t_1, t_2)$, $[t_2, t_3)$ and any $\alpha > 0$, there is a unique $\sigma$ in the space of $C^1$ piecewise cubics with knots $t_1 < t_2 < t_3$ interpolating at $t_1$ with zero ordinate and zero gradient, and at $t_3$ with given ordinate $a$ and slope $M$, which minimizes*

$$Q(s) = \int_{t_1}^{t_3} w(t)[s''(t)]^2\,dt + \alpha[z - s(t_2)]^2,$$

*for any constant $z$. Furthermore,*

$$\lim_{\alpha\to\infty} \sigma(t_2) = z.$$

*Proof.* On differentiating $Q(s)$, we have

$$\begin{cases} \dfrac{\partial Q(s)}{\partial m} = 2\int_{t_1}^{t_3} ws'' \dfrac{\partial s''}{\partial m}\, dt \\ \dfrac{\partial Q(s)}{\partial b} = 2\int_{t_1}^{t_3} ws'' \dfrac{\partial s''}{\partial b}\, dt - 2\alpha(z-b), \end{cases}$$

and so, for an extremum, we obtain

$$\begin{cases} b[\int_{t_1}^{t_3} w(\phi_2'')^2\, dt + \alpha] + m\int_{t_1}^{t_3} w\psi_2''\phi_2''\, dt \\ \qquad = -[\int_{t_1}^{t_3} wa\phi_3''\phi_2''\, dt + \int_{t_1}^{t_3} wM\psi_3''\phi_2''\, dt] + \alpha z, \\ b\int_{t_1}^{t_3} w\phi_2''\psi_2''\, dt + m\int_{t_1}^{t_3} w(\psi_2'')^2\, dt \\ \qquad = -[\int_{t_1}^{t_3} wa\phi_3''\psi_2''\, dt + \int_{t_1}^{t_3} wM\psi_3''\psi_2''\, dt]. \end{cases}$$

Putting

(5.2)
$$A = \int_{t_1}^{t_3} w(\phi_2'')^2\, dt, \qquad D = \int_{t_1}^{t_3} w(\psi_2'')^2\, dt,$$
$$B = \int_{t_1}^{t_3} w\phi_2''\psi_2''\, dt, \qquad E = \left[\int_{t_1}^{t_3} wa\phi_3''\psi_2''\, dt + \int_{t_1}^{t_3} wM\psi_3''\psi_2''\, dt\right],$$
$$C = \left[\int_{t_1}^{t_3} wa\phi_3''\phi_2''\, dt + \int_{t_1}^{t_3} wM\psi_3''\phi_2''\, dt\right],$$

we have, for a critical point,

$$\begin{bmatrix} A+\alpha & B \\ B & D \end{bmatrix}\begin{bmatrix} b \\ m \end{bmatrix} = \begin{bmatrix} \alpha z - C \\ -E \end{bmatrix},$$

and the solution is

(5.3)
$$b = \frac{\begin{vmatrix} \alpha z - C & B \\ -E & D \end{vmatrix}}{\begin{vmatrix} A+\alpha & B \\ B & D \end{vmatrix}} =: \frac{\mathcal{N}(\alpha)}{\mathcal{D}(\alpha)},$$
$$m = -\frac{\begin{vmatrix} \alpha z - C & A+\alpha \\ -E & B \end{vmatrix}}{\begin{vmatrix} A+\alpha & B \\ B & D \end{vmatrix}} =: \frac{\mathcal{M}(a)}{\mathcal{D}(a)},$$

provided $\mathcal{D}(\alpha) \neq 0$. But $\mathcal{D}(\alpha)$ is, save for a positive factor, the Hessian of the quadratic form $Q(s)$. Since $D > 0$, and by the Cauchy-Schwarz inequality, $AD \geq B^2$, we have

$$\mathcal{D}(\alpha) = AD + \alpha D - B^2 > 0.$$

The sufficient conditions for a minimum are that the diagonal entries of $\mathcal{D}(\alpha)$ also be positive, and clearly $\alpha > 0$ implies $A + \alpha > 0$. The coefficient of $\alpha$ in $\mathcal{N}(\alpha)$ is $zD$, and in $D(\alpha)$ it is $D$, so

$$\lim_{\alpha \to \infty} b = z,$$

independently of the weight function. □

It is possible and useful to describe this smoothing spline by characterizing its discontinuities in a way which is reminiscent of the properties of weighted splines demonstrated in [**2**]. As in Proposition 5.1, we now derive necessary conditions satisfied by a smoothing spline $\sigma$ interpolating at $t_1$ with zero value and gradient, and at $t_3$ with value $a$ and slope $M$. At $t_2$ the optimal spline $\sigma$ has a value $b$ and a slope $m$ which depend on the parameters $\alpha$ and $z$.

The penalized energy is a positive definite functional, say $Q$, defined by a bivariate functional $F$ with some parameters $w$ and $\alpha$. So,

$$Q(s) := \int_{t_1}^{t_3} w(t)[D^2 s(t)]^2 \, dt + \alpha(s(t_2) - z)^2 = F(s, s).$$

Here,

$$F(u, v) := \int_{t_1}^{t_3} w(t) D^2 u(t) D^2 v(t) \, dt + \alpha(u(t_2) - z)(v(t_2) - z).$$

$F(u, v)$ has the form $F(u, v) = (u, v) + \alpha(u(t_2) - z)(v(t_2) - z)$, where $(u, v)$ is a semi-inner product and the derivatives are interpreted distributionally. Now $s = \sigma + \beta\psi_2$ is amongst the candidates for $\sigma$, and

$$\begin{aligned} 0 \leq Q(s) &= (s, s) + \alpha(s(t_2) - z)^2 \\ &= (s - \sigma + \sigma, s - \sigma + \sigma) + \alpha(\sigma(t_2) - z)^2 \\ &= (s - \sigma, s - \sigma) + 2(s - \sigma, \sigma) + (\sigma, \sigma) + \alpha(\sigma(t_2) - z)^2 \\ &= Q(\sigma) + \|\beta\psi_2\|^2 + 2\beta(\psi_2, \sigma). \end{aligned}$$

Since $Q(\sigma) \le Q(s)$ for all values of $\beta$, a necessary condition for $\sigma$ to be best is

$$(\psi_2, \sigma) = 0. \tag{5.4}$$

Another necessary condition arises from the fact that $s = \sigma + \gamma\phi_2(s)$ is also a candidate, and a calculation similar to the one above yields

$$\begin{aligned} 0 \le Q(s) &= (s,s) + \alpha(s(t_2) - z)^2 \\ &= (s - \sigma + \sigma, s - \sigma + \sigma) + \alpha(b + \gamma\phi_2(t_2) - z)^2 \\ &= (s - \sigma, s - \sigma) + 2(s - \sigma, \sigma) + (\sigma, \sigma) + \alpha(b - z)^2 \\ &\quad + \alpha[\gamma^2 + 2\gamma(b - z)] \\ &= Q(\sigma) + \gamma^2[\|\phi_2\|^2 + \alpha] + 2\gamma[(\phi_2, \sigma) + \alpha(b - z)]. \end{aligned} \tag{5.5}$$

A second necessary condition is, therefore,

$$(\phi_2, \sigma) + \alpha(b - z) = 0. \tag{5.6}$$

Alternatively, by calculus of variations techniques, for the first condition we have

$$\begin{aligned} \frac{\partial Q(s)}{\partial \beta} &= \frac{\partial}{\partial \beta}[\|\beta\psi_2\|^2 + 2\beta(\psi_2, \sigma)] \\ &= 2\beta\|\psi_2\|^2 + 2(\psi_2, \sigma). \end{aligned}$$

Setting $\beta = 0$ we get (5.4). For (5.5), a similar computation yields (5.6).

**Proposition 5.2.** *For any $C^1$ piecewise cubic $s$ with knots $t_1 < t_2 < t_3$,*

$$-(\psi_2, s) = w(t_2^+)D^2 s(t_2^+) - w(t_2^-)D^2 s(t_2^-)$$

*and*

$$(\phi_2, s) = w(t_2^+)D^3 s(t_2^+) - w(t_2^-)D^3 s(t_2^-).$$

*Proof.* Integrating by parts, we obtain

$$(\psi_2, s) = [w(t)D^2 s(t) D\psi_2(t)]_{t_1}^{t_3} - \int_{t_1}^{t_3} D[w(t)D^2 s(t)] D\psi_2(t)\, dt.$$

The first term in brackets vanishes because $D\psi_2(t_1) = D\psi_2(t_3) = 0$. Derivatives of order three now have to be interpreted distributionally. We are assuming that $w$ is piecewise constant, with a jump discontinuity only at $t_2$. Therefore, $wD^2s$ has a potential jump discontinuity of magnitude $[wD^2s]_2 := w(t_2^+)D^2s(t_2^+) - w(t_2^-)D^2s(t_2^-)$ at $t_2$ and $wD^2s$ is piecewise linear while $D\psi_2$ is continuous. We therefore have

$$\begin{aligned}(\psi_2, s) &= -\int_{t_1}^{t_3} \left[\frac{dw(t)s''(t)}{dt} + [wD^2s]_2\delta(t-t_2)\right] D\psi_2(t)\,dt \\ &= -\int_{t_1}^{t_3} \frac{dw(t)s''(t)}{dt} D\psi_2(t)\,dt - [wD^2s]_2 D\psi_2(t_2).\end{aligned}$$

Here $(dw(t)s''(t)/dt)$ is the ordinary derivative of a piecewise linear function and has a potential jump of some size $[wD^3s]_2 := w(t_2^+)D^3s(t_2^+) - w(t_2^-)D^3s(t_2^-)$ at $t_2$. Using the facts that $D\psi_2(t_2) = 1$ and $\psi_2(t_1) = \psi_2(t_2) = \psi_2(t_3) = 0$ we get, by one more integration by parts,

$$\begin{aligned}(\psi_2, s) &= -\left[\frac{dw(t)s''(t)}{dt}\psi_2(t)\right]_{t_1}^{t_3} \\ &\quad + \int_{t_1}^{t_3} [wD^3s]_2\delta(t-t_2)\psi_2(t)\,dt - [wD^2s]_2 \\ &= -[wD^2s]_2.\end{aligned}$$

For the other condition we compute

$$\begin{aligned}(\phi_2, s) &= \int_{t_1}^{t_3} w(t)D^2\phi_2(t)D^2s(t)\,dt \\ &= [w(t)D^2s(t)D\phi_2(t)]_{t_1}^{t_3} - \int_{t_1}^{t_3} D[w(t)D^2s(t)]D\phi_2(t)\,dt.\end{aligned}$$

Again, the first term vanishes because $D\phi_2(t_1) = D\phi_2(t_3) = 0$. Then

$$\begin{aligned}(\phi_2, s) &= -\int_{t_1}^{t_3} \left[\frac{dw(t)s''(t)}{dt} + [wD^2s]_2(t-t_2)\right] D\phi_2(t)\,dt \\ &= -\left[\frac{dw(t)s''(t)}{dt}\phi_2(t)\right]_{t_1}^{t_3} + \int_{t_1}^{t_3} [wD^3s]_2\delta(t-t_2)\phi_2(t)\,dt \\ &= [wD^3s]_2,\end{aligned}$$

because $\phi_2(t_2) = 1$ and $D\phi_2(t_2) = 0$. □

**Corollary 5.3.** *The necessary conditions for optimality are*

$$w(t_2^+)D^2s(t_2^+) - w(t_2^-)D^2s(t_2^-) = 0$$

and

$$w(t_2^+)D^3s(t_2^+) - w(t_2^-)D^3s(t_2^-) + \alpha(b - z) = 0. \tag{5.7}$$

**Corollary 5.4.** *The integrals* (5.2) *in the smoothing spline formulation of Proposition* 5.1 *are given in terms of weighted jumps in derivatives* $[wD^2s]_2$ *and* $[wD^3s]_2$ *as follows*:

$$\begin{aligned} &B = -[wD^2\phi_2]_2 = [wD^3\psi_2]_2, && D = -[wD^2\psi_2]_2 > 0,\\ &E = -a[wD^2\phi_3]_2 - M[wD^2\psi_3]_2, &&\\ &A = [wD^3\phi_2]_2 > 0, && C = a[wD^3\phi_3]_2 + M[wD^3\psi_3]_2. \end{aligned}$$

*Proof.* In the first result of Proposition 5.2, put $s = \phi_2, \psi_2, \phi_3$ and $\psi_3$ in succession to obtain $B$, $D$ and $E$. Put $s = \phi_2, \phi_3$ and $\psi_3$ in the second to obtain $A$ and $C$. □

**Corollary 5.5.** *The equations defining the smoothing spline in Proposition* 5.1 *are equivalent to the necessary conditions of Corollary* 5.3.

*Proof.* The equation $Bb + Dm + E = 0$ is just

$$w(t_2^+)D^2\sigma(t_2^+) - w(t_2^-)D^2\sigma(t_2^-) = 0,$$

for $\sigma = b\phi_2 + m\psi_2 + a\phi_3 + M\psi_3$, and the equation $Ab + Bm + C = \alpha(z - b)$ is easily seen to be

$$w(t_2^+)D^3\sigma(t_2^+) - w(t_2^-)D^3\sigma(t_2^-) + \alpha(b - z) = 0. \tag{5.8}$$ □

The weighted jumps are simple to compute for the Hermite basis functions. We list the derivatives involved for future reference. Using $t_2 - t_1 = h$, $t_3 - t_2 = k$, we have

$$
\begin{aligned}
&D^2\phi_2(t_2^-) = -\frac{6}{h^2}, && D^2\phi_2(t_2^+) = -\frac{6}{k^2},\\
&D^2\phi_3(t_2^-) = 0, && D^2\phi_3(t_2^+) = \frac{6}{k^2},\\
&D^3\phi_2(t_2^-) = -\frac{12}{h^3}, && D^3\phi_2(t_2^+) = \frac{12}{k^3},\\
&D^3\phi_3(t_2^-) = 0, && D^3\phi_3(t_2^+) = -\frac{12}{k^3},\\
&D^2\psi_2(t_2^-) = \frac{4}{h}, && D^2\psi_2(t_2^+) = -\frac{4}{k},\\
&D^2\psi_3(t_2^-) = 0, && D^2\psi_3(t_2^+) = -\frac{2}{k},\\
&D^3\psi_2(t_2^-) = \frac{6}{h^2}, && D^3\psi_2(t_2^+) = \frac{6}{k^2},\\
&D^3\psi_3(t_2^-) = 0, && D^3\psi_3(t_2^+) = \frac{6}{k^2}.
\end{aligned}
\tag{5.9}
$$

**5.1. Optimal upper and lower splines.** We now consider a family of smoothing splines defined on a portion of an edge (of the triangulation of the vertices $\mathcal{V}$) that is crossed by the hydrographic net. The family will be controlled by the weight function $w$ and the parameters $\alpha$ and $z$. This will offer a means of simulating the erosion of the terrain originally described by the MNN. For the time being, we are using the special boundary conditions as at the beginning of Section 4. Figure 4 illustrates the context and notation. The edge is parametrized by arc length $t$ in such a way that $t = t_1 = 0$ corresponds to the crossing by the net, $t = t_3 > t_1$ corresponds to an endpoint. We choose $t_2 \in (t_1, t_3)$ and assume that the elevations $z$ and $a$ at $t_2$ and $t_3$, respectively, are positive. It is convenient to normalize the weight function. We choose $w(t_2^-) + w(t_2^+) = 1$.

**Definition 5.6.** The upper spline $\sigma_u$ is a weighted smoothing spline, satisfying end conditions as in Proposition 5.1 at $t_1, t_3$, corresponding to $\alpha = \infty$, and therefore interpolating the elevation $z$ at $t_2$, with

weights $w(t_2^-) = 0$ (on $[t_1, t_2)$), $w(t_2^+) = 1$ (on $[t_2, t_3)$). Denote the corresponding weight function $w_u$.

**Observation.** The weights chosen above make $\sigma_u$ as flat as possible on $[t_2, t_3]$ while satisfying the end conditions at $t_3$ and interpolating the value $z$ at $t_2$. However, $\sigma_u$ is normally not the same as the arc of the MNN on $[t_2, t_3]$. Because we have restricted our class of admissible functions for the smoothing splines, the vanishing of the weight function on $[t_2, t_3]$ does not cause difficulties.

**Definition 5.7.** The lower spline $\sigma_l$ is a weighed smoothing spline on $[t_1, t_3]$ corresponding to $\alpha = 0$, satisfying the end conditions at $t_1, t_3$ as above, and with weights $w(t_2^-) = 1$, $w(t_2^+) = 0$. Denote the corresponding weight function $w_l$.

**Lemma 5.8.** *The lower spline $\sigma_l$ vanishes on $[t_1, t_2]$.*

*Proof.* This spline must satisfy

$$w_l(t_2^+)D^2\sigma_l(t_2^+) - w_l(t_2^-)D_l^2\sigma_l(t_2^-) = 0,$$
$$w_l(t_2^+)D^3\sigma_l(t_2^+) - w_l(t_2^-)D_l^3\sigma_l(t_2^-) = 0.$$

In Hermitian form, $\sigma_l = a\varphi_3 + M\psi_3 + b_l\varphi_2 + m_l\psi_2$. Putting in $w_l(t_2^+) = 0$ and $w_l(t_2^-) = 1$, the conditions become

$$b_l D^2\varphi_2(t_2^-) + m_l D^2\psi_2(t_2^-) = 0,$$
$$b_l D^3\varphi_2(t_2^-) + m_l D^3\psi_2(t_2^-) = 0,$$

because $\varphi_3$ and $\psi_3$ vanish identically on $[t_1, t_2]$. A short calculation using the values of the second derivatives in (5.9) above shows that the determinant of this system does not vanish, and thus the unique solution is $b_l = m_l = 0$. In view of the zero end conditions at $t_1$, the entire segment on $[t_1, t_2]$ must vanish. □

**Lemma 5.9.** *If $MK \leq 3a$, the lower spline $\sigma_l$ is nonnegative on $[t_1, t_3]$.*

*Proof.* Consider the control polygon associated with the representation of $\sigma_l$ in terms of the Bernstein basis. By Lemma 5.8, the control

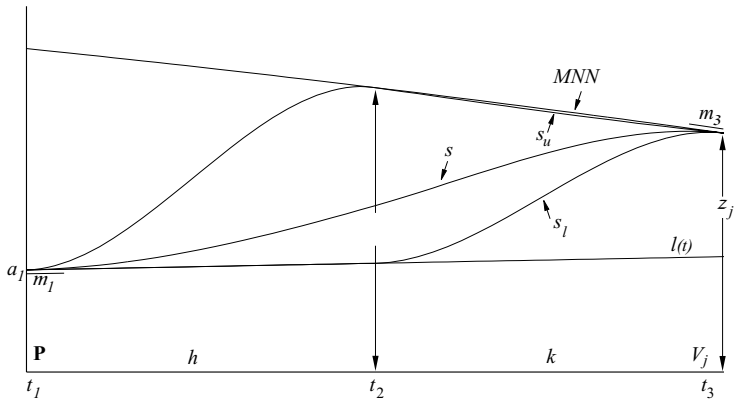


FIGURE 5. The erosion model.

polygon of $\sigma_l$ on $[t_1, t_2]$ has zero ordinates. By $C^1$ continuity, the control polygon on $[t_2, t_3]$ has zero ordinates at $t_2$ and $t_2+k/3$. If $Mk \le 3a$, the ordinate at $t_2 + 2k/3$ is positive, as is the ordinate $a$ at $t_3$. Since $\sigma_l$ lies in the convex hull of its control polygon, $\sigma_l \ge 0$ on $[t_1, t_3]$. □

**6. The erosion model.** Let $e_{ij}$ be an edge of the triangulation that connects vertices $V_i$ and $V_j$ and is crossed once by the hydrographic net at a vertex $\mathbf{P}$ of the net. Consider the portion of this edge connecting $\mathbf{P}$ to $V_j$. Parametrize it by arclength $t$ so that $t = t_1 = 0$ corresponds to $\mathbf{P}$ and $t = t_3 > 0$ corresponds to $V_j$. Let $t_2$ satisfy $t_1 < t_2 < t_3$. There is a cubic arc on $[t_1, t_3]$ originating with the MNN that does not conform to the hydrographic data at $\mathbf{P}$, $t = t_1$. We can construct a family of cubic smoothing splines with knots $t_i$, $i = 1, 2, 3$, that agree with the hydrographic data and share ordinate and slope with the cubic arc of the MNN at $t_3$ as follows. See Figures 4 and 5.

The elevation $a_1$ at $\mathbf{P}$ is known from hydrographic data. The algorithm of Section 3 yields the gradient of the underlying surface $S$ at the vertex $\mathbf{P}$ of $\mathcal{H}$ corresponding to $t_1$. From this we can calculate the directional derivative along $e_{ij}$ and thus obtain $m_1$, the slope of the valley containing the stream. We now reset the datum in such a way that the ordinate and slope at $t_1$ are zero. This we do by subtracting the straight line

$$l(t) := a_1 + m_1(t - t_1) \tag{6.1}$$

from the data. The elevation at the benchmark $V_j$ is now $a := z_j - l(t_3)$. We are assuming that the benchmark elevations are sufficiently larger than those of the net in the sense that $a > 0$. If $m_3$ is the slope obtained from the MNN at $V_j$, we put $M := m_3 - l'(t_3) = m_3 - m_1$. See Figure 5. Given an $\alpha$ and $z$, we can find a smoothing spline $\sigma$ by the method of the previous section. Then the spline $s := \sigma + l$ interpolates the elevation and MNN slope at the benchmark $V_j$, the elevation of the hydrographic net at $\mathbf{P}$, and has an appropriate slope of the valley at $\mathbf{P}$ in the direction of the edge. Furthermore, $s$ is a smoothing spline with the $z$-parameter replaced with $z + l(t_2)$ because then the functional $Q$ of Proposition 5.1 satisfies $Q(\sigma + l) = Q(\sigma)$ and $\sigma + l$ satisfies the jump conditions (5.7) at $t_2$.

We now construct a simple erosion model that uses smoothing splines to modify the original, uneroded MNN profile on an edge to include the presence of the hydrographic net and simulate various degrees of erosion. If $e_{ij}$ is an edge of the triangulation of $\mathbf{P}$ connecting vertices $V_i$ and $V_j$ and containing a vertex $\mathbf{P} = (\xi, \eta)$ of the hydrographic net, we apply Proposition 5.1 and subsequent lemmas and definitions to the two segments from $V_i$ to $\mathbf{P}$ and $\mathbf{P}$ to $V_j$. The initial steps are as follows.

1. Choose one of these segments, say $\mathbf{P}$ to $V_j$, denote its length $l_j$ and parametrize it by arc length $t$ so that

$$\begin{aligned} x(t) &= \left(1 - \frac{t}{l_j}\right)\xi + \frac{t}{l_j}x_j, \\ y(t) &= \left(1 - \frac{t}{l_j}\right)\eta + \frac{t}{l_j}y_j, \end{aligned} \qquad t \in [0, l_j]. \tag{6.2}$$

For a partition $\{0 = t_1 \le t_2 < t_3 = l_j\}$ of $[0, l_j]$, $t = t_1$ and $t = t_3$ will correspond to the vertices $\mathbf{P}$ and $V_j$, respectively. Choose $t_2$. A convenient choice is the midpoint of $[t_1, t_3]$. Verify that $a > 0$ and $Mk \le 3a$, see Lemma 6.9 and recall that $k = t_3 - t_2$. If $\zeta$ is the elevation of the MNN at $t_2$, take $z = \zeta - l(t_2)$ and verify that $z > 0$. Then replace the MNN profile on $[t_1, t_3]$ with a piecewise cubic smoothing spline interpolating and tangent to the MNN at $t = t_3$, interpolating the elevation of the stream with slope $m_1$ at $t = t_1$ and smoothing the MNN profile at $t = t_2$. Satisfaction of the inequalities above ensures that the lower spline $s_l := \sigma_l + l$ lies above $l$ on $[t_1, t_3]$.

2. Repeat the process for the segment $V_i$ to $\mathbf{P}$, reversing its orientation.

In this way we generate a pair of smoothing splines to replace the MNN on the segment $V_iV_j$. Their union is a certain smoothing spline $s$ on that edge. If the data coming from the MNN do not satisfy the inequalities above, an adjustment of the MNN may be required, by addition of elevation data in the vicinity of the hydrographic net, for example.

**Definition 6.1.** An erosion model for an edge of the triangulation crossed by one edge of the hydrographic net is the family of smoothing splines $s$ constructed as above and defined by

1. parameters $(\lambda, \alpha) \in [0,1] \times [0,\infty)$,
2. weight functions linearly interpolated, i.e., $w = (1-\lambda)w_l + \lambda w_u$,
3. a one-to-one mapping $q : [0,1] \to [0,\infty)$ defining $\alpha = q(\lambda)$.

For the time being we do not specify $q$. We would like the family to lie between the upper and lower splines for all values of $\lambda \in [0,1]$ and to deform from the lower to the upper in a monotonic fashion. There are simple ways to do this that do not depend on the minimum energy principle of the smoothing spline. However, since the MNN is based on such a principle, we wish to be consistent with it. While we do not have a full answer to the questions this raises, some results in this direction are proved in this section. They will be obtained for the individuals in the pair making up $s$ so as to simplify notation and will be derived with respect to the datum modified by subtracting the appropriate line $l$. As in (5.9), we put $t_2 - t_1 = h$, $t_3 - t_2 = k$.

Recall that the $b$ of Proposition 5.1 is $\sigma(t_2)$. Hence,

$$\sigma(t_2) = \frac{\begin{vmatrix} \alpha z - C & B \\ -E & D \end{vmatrix}}{\begin{vmatrix} A+\alpha & B \\ B & D \end{vmatrix}} = \frac{\alpha z D + F}{\alpha D + G},$$

where $zD > 0$, $D > 0$, $F = BE - CD$ and $G = AD - B^2 \geq 0$. These depend on the weights, but for any fixed set of weights, $\sigma(t_2)$

changes monotonically from the value $F/G$ corresponding to $\alpha = 0$, to $z$ for $\alpha = \infty$. As a consequence of the linear interpolation of weight functions, we have $w(t_2^-) = 1 - \lambda$, $w(t_2^+) = \lambda$ and a calculation using Corollary 5.4 yields

$$G = \frac{12}{h^4k^4}[(k^2(1-\lambda) + h^2\lambda)^2 + 4\lambda(1-\lambda)(h^3k + h^2k^2 + hk^3)] > 0. \tag{6.3}$$

Also,

$$F = \frac{12\lambda}{h^2k^4}[\lambda h^2(a - Mk) + (1-\lambda)k(a(3k + 4h) - Mk(k + 2h))]. \tag{6.4}$$

Since $\alpha = 0$ corresponds to $\lambda = 0$, $\sigma(t_2) = 0$ when $\alpha = 0$. When $\alpha = \infty$ then $\lambda = 1$ and $\sigma(t_2) = z$. We now show that, under mild hypotheses, $\sigma(t_2) \geq 0$ for all $(\lambda, \alpha) \in [0, 1] \times [0, \infty)$.

**Lemma 6.2.** *If $MK \leq a$, then $\sigma(t_2) \geq 0$.*

*Proof.* The coefficient of $(1 - \lambda)k$ in (6.4) is

$$a(3k + 4h) - Mk(k + 2h) > a(k + 2h) - Mk(k + 2h) \geq 0.$$

Consequently, $F$ is a nonnegative multiple of a linear combination of positive quantities with positive coefficients and hence nonnegative. Since $G > 0$ and $D > 0$, the conclusion follows. □

In view of Definition 5.10,

$$\sigma(t_2) = \frac{q(\lambda)zD + F}{q(\lambda)D + G} = z + \frac{F - zG}{q(\lambda)D + G}. \tag{6.5}$$

Since $q(\lambda)D + G > 0$, $\sigma(t_2) < z$ for $\lambda < 1$ if and only if $F - zG \leq 0$ for all $\lambda \in [0, 1]$, and this is independent of $q(\lambda)$.

Looking at the values of $F$ and $zG$ at the ends of $[0, 1]$, we find

$$(zG - F)(0) = \frac{12z}{h^4} > 0,$$
$$(zG - F)(1) = \frac{12}{k^4}(z - a + kM) \geq 0.$$

The last condition holds only if

$$z \geq a - Mk.$$

It is easy to see that, in terms of the original datum, this condition is

$$\zeta \geq z_j - m_3 k,$$

or, geometrically, that the MNN at $t_2$ is not below the tangent line drawn to the MNN at $t_3$. This is an interesting condition which is related to how well the MNN approximates a reasonable terrain profile on the edge in question, and plays a role in the following lemma concerning the behavior of $\sigma(t_2)$ as a function of $\lambda$.

**Lemma 6.3.** *For fixed $\lambda$, if $z \geq a - Mk$ and $Mk \leq a$, then $\sigma(t_2) < z$ for all $\lambda \in [0, 1)$.*

*Proof.* Notice that $F - ZG$ is a quadratic in $\lambda$. From (6.4), (6.3) and assuming that $z \geq a - Mk$, $(zG - F)' \geq (a - Mk)G' - F'$. For convenience, put $(a - Mk)G' - F' = 12f'(\lambda)$.

If the coefficient of $\lambda^2$ in $zG - F$ is nonpositive, then in view of the nonnegative values of $(a - Mk)G - F$ at $\lambda = 0, 1$, $zG - F \geq 0$ for all $\lambda \in [0, 1]$. If the coefficient is positive, then we impose the condition that the zero of $f'(\lambda)$ is greater than or equal to 1. A calculation with $F$ and $G$ (6.4), (6.3), yields

$$\frac{[-a(-2k^4 + 4hk^3 + 9h^2k^2 + 8h^3k - h^4) + Mk(-2k^4 + 4hk^3 + 7h^2k^2 + 6h^3k - h^4)]}{[a(2k^4 - 8hk^3 - 12h^2k^2 - 8h^3k + 2h^4) - Mk(2k^4 - 8hk^3 - 12h^2k^2 - 8h^3k + 2h^4)]} \geq 1.$$

The denominator is a positive multiple of the positive coefficient of $\lambda^2$ and the above inequality is equivalent to

$$a(4hk^3 + 9h^2k^2 + 8h^3k) - Mk(4hk^3 + 7h^2k^2 + 6h^3k) \geq 0.$$

But

$$\begin{aligned} &a(4hk^3 + 9h^2k^2 + 8h^3k) - Mk(4hk^3 + 7h^2k^2 + 6h^3k) \\ &\quad > a(4hk^3 + 7h^2k^2 + 6h^3k) - Mk(4hk^3 + 7h^2k^2 + 6h^3k) \\ &\quad = (a - Mk)(4hk^3 + 7h^2k^2 + 6h^3k) \geq 0 \end{aligned}$$

if $a - Mk \geq 0$, and indeed the zero of $f'(\lambda)$ is $\geq 1$. The end conditions on $(a - Mk)G - F$ ensure the positivity of $zG - F$ for all $\lambda \in [0, 1]$. □

The following proposition summarizes the properties of the smoothing spline erosion model proved to this point in terms of the original datum. Recall (Figure 5) that $\zeta$ is the elevation of the MNN at a certain point on an edge $e_{ij}$ between a hydrographic net crossing $\mathbf{P}$ and the vertex $V_j$, distant $h$ from $\mathbf{P}$ and $k$ from $V_j$, $z_j$ is the elevation of the MNN at $V_j$ and $m_3$ is the slope of the MNN at $V_j$ in the direction from $\mathbf{P}$ to $V_j$. In the preamble to Lemma 6.3, we pointed out that the condition $z \geq a - Mk$ is equivalent to $\zeta \geq z_j - m_3 k$. A simple calculation shows that $Mk \leq a$ is the same as

$$z_j - m_3 k \geq l(t_2),$$

which has a convenient graphical interpretation and can influence the choice of $t_2$ in the erosion model.

**Proposition 6.4.** *If $\zeta \geq z_j - m_3 k$ and $z_j - m_3 k \geq l(t_2)$, the family of smoothing splines defining the profile of the eroded terrain on $[t_1, t_3]$ according to Definition* 6.1 *has the property that, for any choice of the mapping $q$, the smoothing spline $s$ corresponding to a parameter value $\lambda \in [0, 1]$ satisfies $0 \leq s(t_2) \leq \zeta$. With obvious changes the same results hold for the edge connecting $\mathbf{P}$ to $V_i$.*

The inequality conditions are not very restrictive and represent a reasonable behavior of the MNN on the edge in question. In particular the condition $z_j - m_3 k \geq l(t_2)$ only requires the MNN not to be too steep at the end point of the edge crossed by the hydrographic net. Recall also Lemma 5.9 which guarantees the nonnegativity of the lower spline if $Mk < 3a$ which is certainly true if $Mk \leq a$ or $z_j - m_3 k \geq l(t_2)$. The behavior of the smoothing spline family on the entire interval $[t_1, t_3]$ depends on the choice of $q$ (see Definition 6.1). While we have no proof at this time, it seems that in order to prevent unreasonable oscillations of the profile, $q$ should be chosen so that the low energy of the smoothing spline on $[t_1, t_2]$, represented by the relatively large size of the weight $w_l(t_2^-)$ on that interval, i.e., $\lambda$ close to 0, does not increase

too rapidly as $\alpha$ increases. For the examples that we have computed, our choice was

$$\alpha = \frac{\lambda}{1-\lambda},$$

which has qualitatively the appropriate behavior. We note that the inequalities ensuring reasonable behavior of the family of smoothing splines represent sufficient, rather than necessary, conditions. In a practical application, a violation serves as a warning to the user, and a manual choice of $\lambda$ may resolve any problem with the valley profile.

**7. Blending of the curve network.** As a result of the algorithms of the previous sections, we have a cubic curve network defined on the edges of $\mathcal{E} \cup \mathcal{H}$. These subdivide $\Omega$ into triangular as well as quadrilateral patches. Here we use the blending method described in [**8**] to generate the surface $S$ that we seek. This method applies only to triangles. We will apply it to quadrilaterals by inserting two diagonals and averaging the blended interpolant. The method requires knowledge of $\nabla S$ on the edges. These can be generated by interpolating the known gradients at the vertices. For a quadrilateral patch insert a diagonal. Then the gradient and elevation are known at its end points and a cubic interpolant along the diagonal is uniquely determined. The gradient can be interpolated along the diagonal, and blending can be applied. The same can be done for the other diagonal. To remove bias, we average the two results on the quadrilateral to obtain the final interpolant. In this section we describe a piecewise quadratic interpolant which contains the method used by Nielson [**8**] as a special case. On each edge this interpolant contains a parameter that we will be able to adjust. In particular, on those edges which correspond to the hydrographic net, we will use it to make the gradient of the blended surface as parallel to the direction of the stream as possible in an $L^2$ sense. As the hydrographic net is now incorporated into the original triangulation, we no longer make any notational distinction between vertices and edges originating from the two initial data sets.

Through the construction of the MNN and the erosion model, we have the restrictions of some function $S$ to the edges of a triangulation. In our case these restrictions are cubics. The gradient of $S$ is available at the vertices; denote this $\nabla S_i$ at a vertex $V_i$. The derivative of $S$ along any edge of the triangulation is also known. Consider an edge

$e_{ij}$. Let $\mathbf{e}_{ij}$ be a unit vector along this edge. Parametrize this edge by arclength $t$ and let $l_{ij} = \|e_{ij}\|\}$, the length of the edge. Let $t = 0$ and $t = l_{ij}$ correspond to the vertices $V_i$ and $V_j$, respectively. Put $\mathbf{v} = \mathbf{e}_{ij} + \beta \mathbf{n}_{ij}$ where $\mathbf{n}_{ij}$ is a unit vector perpendicular to $\mathbf{e}_{ij}$ pointing into the interior of the triangle and $\beta$ is a parameter.

**Proposition 7.1.** *On every edge $e_{ij}$, a one-parameter family of quadratic interpolants of the gradient of $S$ exists that can be written in the form*

$$\mathbf{Q}(t) = \mathbf{L}(t) + \alpha t(l_{ij} - t)\mathbf{v}, \tag{7.1}$$

*where $\mathbf{L}(t)$ is the linear interpolant of the gradient given by* (7.3) *and $\alpha$ is given by*

$$\alpha = 6/l_{ij}^2(C - T). \tag{7.2}$$

*Here $T$ denotes the tangential (scalar) component of the mean of the gradients at the ends of the edge, and $C$ is the slope of the chord joining $V_i$ to $V_j$.*

*Proof.* Because $S$ is cubic on this edge, its derivative along the edge is a known quadratic, say $(dS/dt) = q_{ij}(t)$. It must be true that $\nabla S_i \bullet \mathbf{e}_{ij} = q_{ij}(0)$ and $\nabla S_j \bullet \mathbf{e}_{ij} = q_{ij}(l_{ij})$. We seek a gradient $\nabla S$, defined on $e_{ij}$ such that $\nabla S \bullet \mathbf{e}_{ij} = q_{ij}(t)$. Let us interpolate $\nabla S$ along the edge by a quadratic. Such a quadratic is not unique. Let $\mathbf{L}$ be the linear interpolant of the gradients at $V_i, V_j$. Then

$$\mathbf{L}(t) = \left(1 - \frac{t}{l_{ij}}\right)\nabla S_i + \frac{t}{l_{ij}}\nabla S_j, \tag{7.3}$$

and, for each constant $\alpha$ and constant vector $\mathbf{v} \neq \mathbf{0}$, one has the family of quadratic interpolants

$$\mathbf{Q}(t) = \mathbf{L}(t) + \alpha t(l_{ij} - t)\mathbf{v}.$$

An exceptional case occurs if $q_{ij}(t)$ is in fact linear. Then $\alpha = 0$ and $\mathbf{L}(t)$ reproduces it. Suppose $\alpha \neq 0$. The derivative of $S$ along the edge is $\mathbf{Q} \bullet \mathbf{e}_{ij} = \mathbf{L} \bullet \mathbf{e}_{ij} + \alpha t(l_{ij} - t)\mathbf{v} \bullet \mathbf{e}_{ij} = \mathbf{L} \bullet \mathbf{e}_{ij} + \alpha t(l_{ij} - t)$, a quadratic

in $t$, say $p(t)$. $\mathbf{L} \bullet \mathbf{e}_{ij}$ is linear in $t$ and, because $\mathbf{L}$ interpolates $\nabla S$, we have $p(0) = \nabla S_i \bullet \mathbf{e}_{ij} = q_{ij}(0)$ and $p(l_{ij}) = \nabla S_j \bullet \mathbf{e}_{ij} = q_{ij}(l_{ij})$. Now we make $p(l_{ij}/2) = q_{ij}(l_{ij}/2)$. This gives

$$\mathbf{L}\left(\frac{l_{ij}}{2}\right) \bullet \mathbf{e}_{ij} + \frac{l_{ij}^2}{4}\alpha = q_{ij}\left(\frac{l_{ij}}{2}\right),$$

and

$$\alpha = \frac{4}{l_{ij}^2}\left[q_{ij}\left(\frac{l_{ij}}{2}\right) - \mathbf{L}\left(\frac{l_{ij}}{2}\right) \bullet \mathbf{e}_{ij}\right]. \tag{7.4}$$

Note that $\alpha$ is independent of the parameter $\beta$. If the cubic $S$ is degenerate, it is possible that $\alpha = 0$.

Because $p(t)$ and $q_{ij}(t)$ are both quadratics which coincide at three distinct points, they must be identical. With the above value of $\alpha$, $\mathbf{Q}$ is a quadratic interpolant of the gradient along the edge consistent with the derivative along the edge obtained from the curve network. Clearly, the solution is not unique because of the arbitrariness in $\mathbf{v}$ coming from $\beta$. Now observe (7.3) that

$$\mathbf{L}\left(\frac{l_{ij}}{2}\right) = \frac{\nabla S_i + \nabla S_j}{2},$$

and thus $T := \mathbf{L}(l_{ij}/2) \bullet \mathbf{e}_{ij}$ is the tangential (scalar) component of the mean of the gradients at the ends of the edge. A short calculation with the Hermite form of the cubic along the edge shows that

$$q_{ij}\left(\frac{l_{ij}}{2}\right) = \frac{3}{2l_{ij}}[S(V_j) - S(V_i)] - \frac{T}{2}.$$

But $C := [S(V_j) - S(V_i)]/l_{ij}$ is the slope of the chord joining $V_i$ to $V_j$. We conclude that

$$\alpha = \frac{6}{l_{ij}^2}(C - T). \qquad \square$$

From the equation (7.1)

$$\nabla S = \left(1 - \frac{t}{l_{ij}}\right)\nabla S_i + \frac{t}{l_{ij}}\nabla S_j + \alpha t(l_{ij} - t)[\mathbf{e}_{ij} + \beta \mathbf{n}_{ij}],$$

we find that the interpolated value of the derivative normal to the edge is

$$\begin{aligned}\nabla S \bullet \mathbf{n}_{ij} &= \left[\left(1 - \frac{t}{l_{ij}}\right)\nabla S_i + \frac{t}{l_{ij}}\nabla S_j\right] \bullet \mathbf{n}_{ij} + \alpha\beta t(l_{ij} - t) \\ &= \mathbf{L}(t) \bullet \mathbf{n}_{ij} + \alpha\beta t(l_{ij} - t).\end{aligned}$$

Here we see that, if $\beta = 0$, then this is equivalent to linear interpolation of the derivative normal to the edge. In what we call Nielson's method, one makes the choice $\beta = 0$ on all edges.

If $e_{ij}$ is an edge corresponding to the hydrographic net, then the gradient there should be parallel to the edge. That means that the derivative normal to the edge should be zero. While $\alpha$ is already determined, we would like to choose $\beta$ so that this quantity is as close to zero on the edge as possible. One measure of this is the $L^2$-norm. We therefore minimize

$$\|\nabla S \bullet \mathbf{n}_{ij}\|^2 = \int_0^{l_{ij}} [\mathbf{L}(t) \bullet \mathbf{n}_{ij} + \alpha\beta t(l_{ij} - t)]^2 \, dt.$$

Let $T, C$ be as in Proposition 7.1, and let $N := ((\nabla S_i + \nabla S_j)/2) \bullet \mathbf{n}_{ij}$ denote the normal (scalar) component of the mean of the gradients at the ends of the edge.

**Proposition 7.2.** *When $\alpha \neq 0$, $\|\nabla S \bullet \mathbf{n}_{ij}\|^2$ is least if*

$$\beta = \frac{5}{6}\frac{N}{T - C}.$$

*Proof.*

$$\|\nabla S \bullet \mathbf{n}_{ij}\|^2 = \int_0^{l_{ij}} [\mathbf{L}(t) \bullet \mathbf{n}_{ij} + \alpha\beta t(l_{ij} - t)]^2 \, dt.$$

Now

$$\frac{\partial}{\partial\beta}\|\nabla S \bullet \mathbf{n}_{ij}\|^2 = 2\alpha \int_0^{l_{ij}} [\mathbf{L}(t) \bullet \mathbf{n}_{ij} + \alpha\beta t(l_{ij} - t)]t(l_{ij} - t) \, dt.$$

Since the coefficient of $\beta^2$ in $\|\nabla S \bullet \mathbf{n}_{ij}\|^2$ is positive, the optimal value of $\beta$ is

$$\begin{aligned}\beta &= -\int_0^{l_{ij}} [\mathbf{L}(t) \bullet \mathbf{n}_{ij}] t(l_{ij} - t)\, dt \Big/ \alpha \int_0^{l_{ij}} t^2 (l_{ij} - t)^2\, dt \\ &= \frac{30}{\alpha l_{ij}^5} \int_0^{l_{ij}} [\mathbf{L}(t) \bullet \mathbf{n}_{ij}] t(t - l_{ij})\, dt.\end{aligned}$$

Using (7.3) we have

$$\int_0^{l_{ij}} \mathbf{L}(t) t(t - l_{ij})\, dt = -\frac{l_{ij}^3}{12}(\nabla S_i + \nabla S_j).$$

Consequently,

$$\int_0^{l_{ij}} \mathbf{L}(t) \bullet \mathbf{n}_{ij} t(t - l_{ij})\, dt = -\frac{l_{ij}^3}{6}\left(\frac{\nabla S_i + \nabla S_j}{2}\right) \bullet \mathbf{n}_{ij} = -\frac{l_{ij}^3 N}{6},$$

and

$$\beta = -\frac{5N}{\alpha l_{ij}^2}.$$

However, recall (7.4) that $\alpha = 6(C - T)/l_{ij}^2$. The result follows. □

If the MNN along the edge is linear, then $T = C$. Then $\alpha = 0$ and we do not compute $\beta$ in this way. It is arbitrary, and for this application we choose $\beta = 0$. Thus,

$$\beta = \begin{cases} \dfrac{5}{6}\dfrac{N}{T - C} & T \neq C, \\ 0 & T = C. \end{cases} \tag{7.5}$$

Discretion is advised due to rounding errors in borderline situations.

**8. Examples.** For the purpose of illustration the above results, we chose a set $\mathcal{B}$ of 9 benchmark points from a topographical map, Figure 10, and a set of 11 points of the hydrographic net contained in the convex hull of $\mathcal{B}$, as illustrated in Figures 1 (a), (b), (c) and 10. The computations for these, and subsequent figures, were carried out

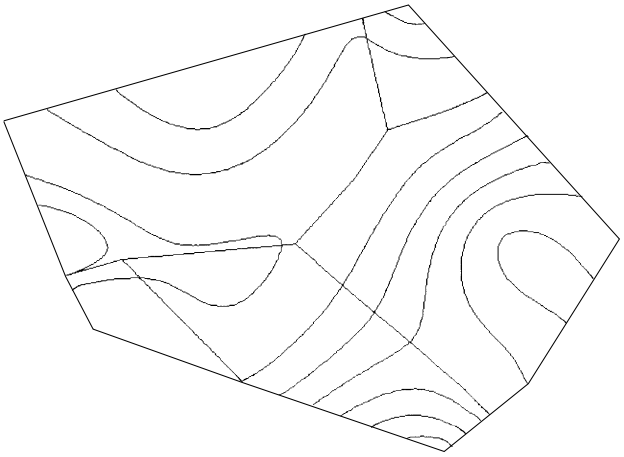

FIGURE 6. A thin-plate spline interpolant.

with the aid of Maple V. Additional work on the figures was done with Corel Draw 7 by `www.Highpointdesigns.com`.

A spline minimum norm network (MNN) was constructed over the edges of the triangulation and is shown in Figure 2. In order to include the presence of the hydrographic net, the MNN profiles intersected by $\mathcal{H}$ were modified by the methods described in Section 5, initially using $\lambda = 0.7$ and $t = l/2$ (see Proposition 5.4).

Figure 6 is a thin-plate spline interpolant of the 20 initial points. The net $\mathcal{H}$ is also shown. As expected, the surface is very smooth, but poorly approximates the important features of the original. Figure 7 is a contour map of the surface produced by the blending method described by Nielson [**8**] with $\alpha$ determined from (7.2) and $\beta = 0$. In some regions one can see substantial deviations of the direction of the gradient vector on $\mathcal{H}$ from the direction of $\mathcal{H}$. This has especially serious consequences in the southeastern part of the map where cuspiness in the contours on a triangulation edge near the stream appears to be due to a poor gradient on the stream. Figure 8 was produced with an optimized (7.5) on edges coming from $\mathcal{H}$. There is a clear difference between these two pictures. In the latter the contours in the stream in the southeast are more rounded, and the contours in the west are more orthogonal to the hydrographic net. There is some roughness in the surfaces, inherited from the triangulation and the blending method employed.

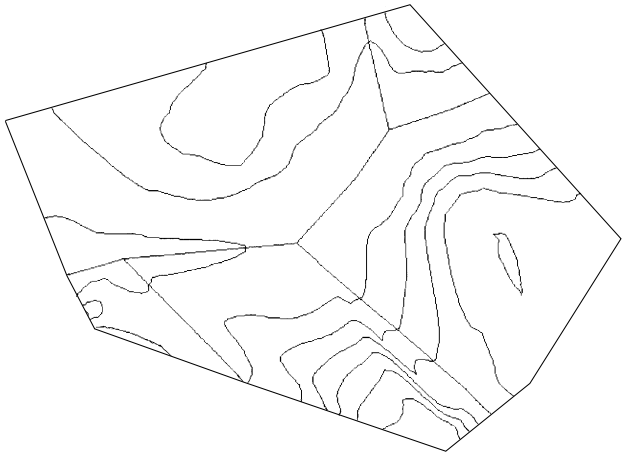

FIGURE 7. Nielson's blending.

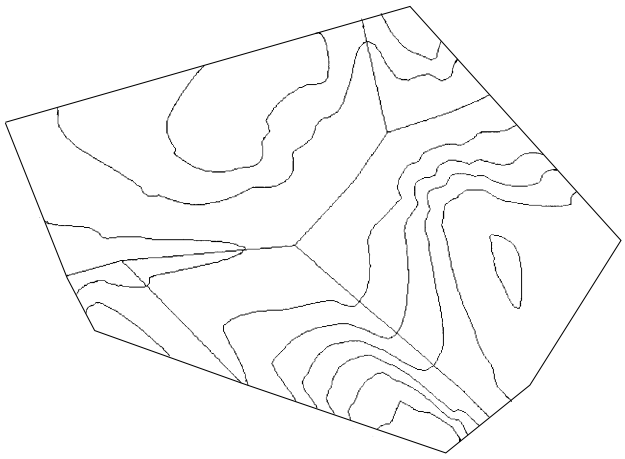

FIGURE 8. Blending with optimal beta.

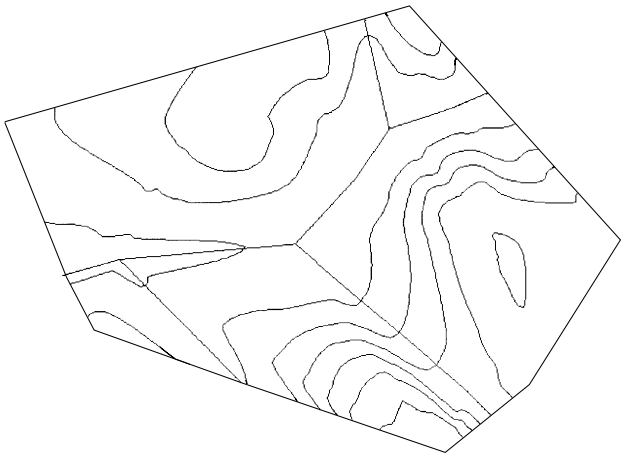

FIGURE 9. Adjusted map.

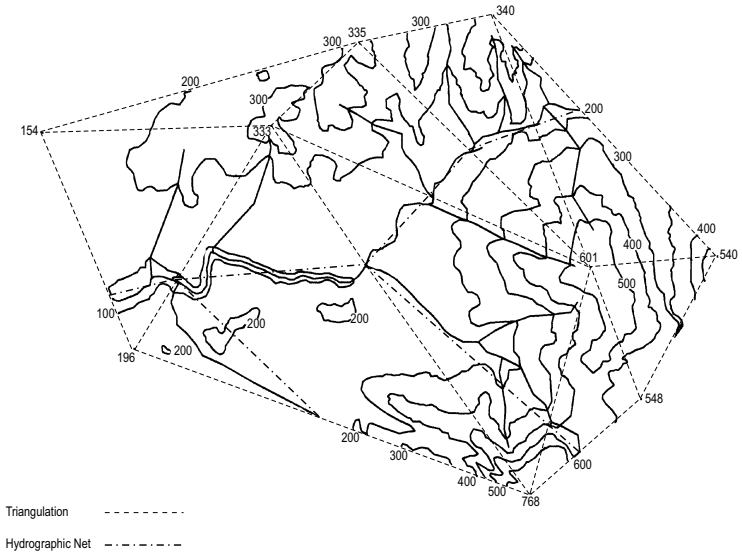


FIGURE 10. Original contour map.

Some smoothing may be possible by adjusting $\beta$ on some additional edges. Figure 9 is a map in which the original value $\lambda = 0.7$ and $t_2$ has been changed in a few places to improve valley profiles in the blended surface. In particular, the valley in the eastern part of the map has been narrowed on the south side so as to conform more closely to Figure 10, which is the contour map from which the data was derived.

For a practical application of the methods discussed above, it is necessary to study further the impact of the various parameters available in the erosion model and to deal effectively with the problems of insertion of additional data.

**9. Acknowledgments.** We thank the referee for helpful comments. The second author is grateful to the University of Calgary for provision of research facilities in view of his emeritus position there.

## REFERENCES

**1.** D. Apprato and R. Arcangéli, *Adjustement spline long d'un ensemble de courbes*, RAIRO Modél. Math. Anal. Numér. **25** (1991), 193–212.

**2.** L.P. Bos and K. Šalkauskas, *Weighted splines based on piecewise polynomial weight functions*, in *Curve and surface design* (*Tempe, AZ, 1989*), Geom. Des. Publ., SIAM, Philadelphia, (1992), Ch. 5, 87–98.

**3.** P. Cinquin, *Splines Unidimensionelles Sous Tension et Bidimensionelles Parametrées*: *Deux Applications Medicales*, Thèse, Université de Saint-Etienne, 1981.

**4.** F.N. Fritsch and R.E. Carlson, *Monotone piecewise cubic interpolation*, SIAM J. Numer. Anal.**17** (1980), 238–246.

**5.** D. Holland, *Generalized minimum norm networks*, Ph.D. Thesis, Univ. of Calgary, 1993.

**6.** P-J. Laurent,*Approximation et Optimization*, Hermann, Paris, 1972.

**7.** G.M. Nielson, *The side-vertex method for interpolation in triangles*, J. Approx. Theory **25** (1979), 318–336.

**8.** ———, *A method for interpolating scattered data based upon a minimum norm network*, Math. Comp. **40** (1983), 253–271.

**9.** H. Pottman, *Interpolation on surfaces using minimum norm networks*, Comput. Aided Geom. Design **9** (1992), 51–67.

**10.** E. Puppo, L. Davis, D. de Menthon and Y.A. Teng, *Parallel terrain triangulation*, Internat. J. Geograph. Info. Sci. **8** (1994), 105–128.

**11.** K. Šalkauskas, $C^1$ *splines for interpolation of rapidly varying data*, Rocky Mountain J. Math. **14** (1984), 239–250.

**12.** G. Wahba, *Spline models for observational data*, SIAM Stud. Appl. Math. **59**, 1990.

University of Coimbra, 3000 Coimbra, Portugal
*E-mail address:* leonor@mat.uc.pt

University of Calgary, Calgary, Alberta T2N 1N4, Canada
*E-mail address:* ksalkaus@ucalgary.ca